Microwave atomic force microscopy imaging for nanometer-scale electrical property characterization

Lan Zhang, Yang Ju,[a] Atsushi Hosoi, and Akifumi Fujimoto
Department of Mechanical Science and Engineering, Nagoya University, Furo-Cho, Chikusa-ku, Nagoya 4648603, Japan

(Received 4 September 2010; accepted 15 November 2010; published online 30 December 2010)

We introduce a new type of microscopy which is capable of investigating surface topography and electrical property of conductive and dielectric materials simultaneously on a nanometer scale. The microwave atomic force microscopy is a combination of the principles of the scanning probe microscope and the microwave-measurement technique. As a result, under the noncontact AFM working conditions, we successfully generated a microwave image of a 200-nm Au film coating on a glass wafer substrate with a spatial resolution of 120 nm and a measured voltage difference of 19.2 mV between the two materials. © *2010 American Institute of Physics*. [doi:10.1063/1.3525058]

I. INTRODUCTION

Electrical properties are the most significant intrinsic characteristics of substances and strongly affect the work functions of different materials, especially in nanometer-scale materials and devices. Thus, the evaluation of electrical properties is a very important issue when investigating the physical properties of nanometer-scale materials and devices. Atomic force microscopy[1,2] (AFM) is a well known and powerful technique, which has an irreplaceable role in nano science and technology, because of its unique ability to image and manipulate surface structures on the nanometer scale.[3–6] To characterize the electrical features of materials on the nanometer scale, extended techniques based on AFM, such as Kelvin probe force microscopy (KFM),[7,8] scanning capacitance microscopy (SCM),[9,10] conducting atomic force microscopy (C-AFM),[11,12] and electrostatic force microscopy (EFM),[13,14] have been developed over time. Although, KFM can measure the surface electrical potential of materials by detecting the electrostatic force between the probe tip and the sample, electrostatic forces, including van der Waals forces and chemical bonding forces, are also included in the measured data; hence, sample surface chemistry and atmospheric conditions greatly impact the measured potential. Scanning capacitance microscopy can characterize electrical information by measuring the capacitance between the tip of the probe and the sample; however, it suffers from a limited spatial resolution and is sensitive to specimen thickness. Electrostatic force microscopy can probe local charge distributions on surfaces with a satisfactory spatial resolution; however, the tip must scan the sample surface twice: one time for the surface topography measurement and the second for electrical information. The accuracy of the dual-pass scanning technique is greatly impacted by probe drifts during the second scan. On the other hand, microwave measurement has been of a great interest to many researchers because microwaves can propagate well in air and the sample's response is directly related to the electrical properties of the materials.[15,16] Thus, to obtain microscopic electrical information, a variety of microwave measurement-based microscopic methods have been developed, more specifically, scanning evanescent microwave microscopy (SEMM),[17,18] and near-field scanning microwave microscope (NSMM).[19–21] Among these techniques, it is important to note that the measured signals will be affected by the standoff distance between the probe tip and the sample, thus, obtaining the absolute electrical characteristic information is difficult. To summarize, these AFM-based methodologies and microwave microscopy can only image relative electrical properties, and they are unable to measure the absolute values of the intrinsic electrical properties, such as conductivity, permittivity, and permeability. Microscopy that can provide a simultaneous measurement of topography and electrical properties on a nanometer scale is still being developed.

Recently, to solve the problem that microwave signals are affected by the standoff distance, the technique to combine the microwave microscopy with AFM has been studied.[22–26] Weide group combined NSMM with a commercial AFM together,[23,24] in order to obtain the AFM topography and microwave image of a sample simultaneously. Shen and co-workers invented a microwave impedance microscope[25,26] (MIM) which fed a microwave signal to a traditional AFM probe. It can also be used to sense the electronic properties of measured samples. However, it is noted that NSMM-AFM and MIM do not use matched probe and cantilever as the microwave-guide connected with the source of microwave signals. Thus, the microwave signals may not propagate along the probe and emit from the tip apex of the probe. Therefore, these techniques can only measure the impedances changes of the probe-sample system but not the intrinsic electrical properties, such as conductivity, permittivity, and permeability. In this paper, we demonstrate a novel microwave atomic force microscopy (M-AFM) technique that maintains a constant standoff distance in an AFM measurement and quantitatively evaluates the electrical properties of materials with a microwave instrument. The M-AFM probe is operated in air in a noncontact mode. By combining the advantages of AFM with microwave-based measurement,

[a]Author to whom correspondence should be addressed. Electronic mail: ju@mech.nagoya-u.ac.jp. Tel.: +81-52-789-4672. Fax: +81-52-789-3109.

0034-6748/2010/81(12)/123708/4/$30.00 © 2010 American Institute of Physics

Author complimentary copy. Redistribution subject to AIP license or copyright, see http://rsi.aip.org/rsi/copyright.jsp

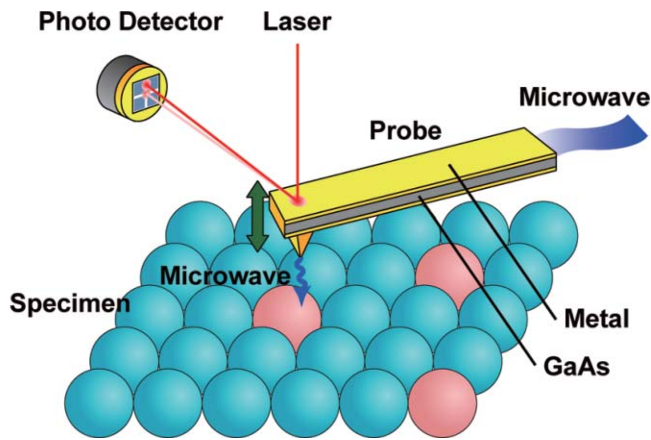

FIG. 1. (Color online) Schematic diagram of the M-AFM probe that was used to measure the electrical properties of materials in this study.

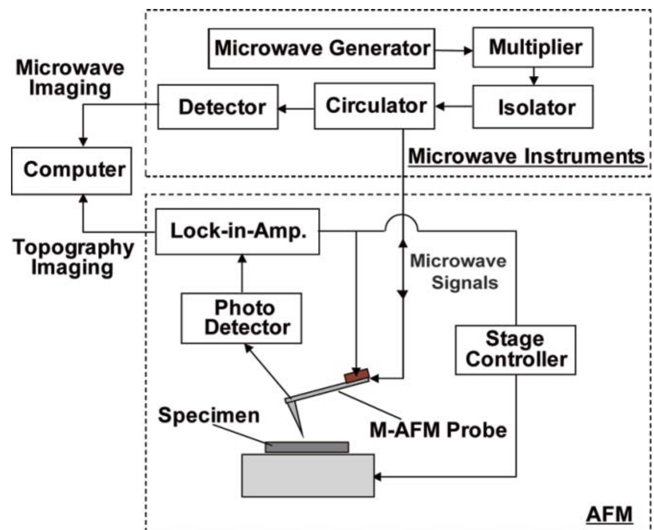

FIG. 2. Diagram of the M-AFM system.

topographical imaging with a high spatial resolution and the *in situ* measurement of nanometer-scale electrical properties can be realized. As can be observed in Fig. 1, the M-AFM probe consists of a homogeneous parallel-plate (the metal films are located on the top and bottom surfaces of the probe) and a nano-slit that is across the tip apex. These special structures allow microwave signals to propagate through the probe and emit from the tip of the M-AFM probe. When the M-AFM probe is located above a sample surface, the nano-slit on the tip acts as a source of microwave signals that transmit into the surface of the sample and as a receiver of the microwave signals that reflect from the measured sample. By analyzing the measured reflection signals, the electrical information of the measured materials can be determined.

In previous studies, M-AFM probes have enabled us to measure the topography of a grating sample with high resolution in air in the noncontact AFM mode.[27] These results demonstrate that the M-AFM probe has a similar ability to image the surface topography of materials in comparison with a conventional Si AFM probe. To confirm the emission of microwaves at the tip of the M-AFM probe, a network analyzer was connected to the M-AFM probe by a coaxial line.[28] When the test samples approached the tip of probe, the reflected microwave signals were measured by the network analyzer, which indicates that the nano-slit at the tip of probe can act as a sensor to emit and receive microwave signals. Moreover, the effects of using Al and Au as waveguide coating materials for the propagation of microwave signals in the M-AFM probe has also been studied.[29] However, because it is difficult to synchronize the network analyzer that is used to measure the microwave signals with the AFM scanner that is used to create the AFM image, a microwave AFM image has not yet been achieved. Therefore, in this study a compact microwave instrument was constructed which can be appropriately synchronized with an AFM scanner. Consequently, a microwave AFM image was realized.

II. EXPERIMENTAL SETUP

Figure 2 schematically depicts the integrated test system of the M-AFM. In our M-AFM system, the initial microwave signals, which are working at a frequency $f = 16.66$ GHz, are generated by a microwave generator. Next, the frequency of the microwave signals is extended by a six-frequency multiplier, which results in a stable testing frequency $f = 94$ GHz. The microwave signals propagate through an isolator and a circulator and then propagate into the M-AFM probe. The transmission line that connects the circulator and the probe changes from a rectangular waveguide into a coaxial line, which then changes into the parallel-plate waveguide (in the M-AFM probe). A detector is connected to the circulator, to measure the microwave signals that are received by the tip of the probe and indicate the voltage data that are converted from the reflected microwave signals. The measured signals are synchronized with positional information that is obtained from the AFM scanner, which is then used to create a microwave image. At the same time, by evaluating the output voltage data, the electrical properties of the measured materials can be determined.

To reduce the attenuation of microwaves that propagate in the M-AFM probe and obtain a desired structure, we elected to use an undoped GaAs wafer as the substrate of the M-AFM probe.[30,31] Wet etching was used to fabricate the probe because, unlike dry etching techniques, side etching occurs under the resist pattern during the wet etching, which permits the realization of a microfabricated pyramidal GaAs tip. To facilitate proper microwave signal propagating through the probe, a parallel-plate waveguide was formed by evaporating Au films onto the top and bottom surfaces of the M-AFM probe. The Au films on both sides are connected at the end of the probe cantilever, and there are no Au films on the sides of the cantilever and probe body. To make microwave signals emit from the apex of the probe tip, a nano-slit at the tip of the probe was fabricated via a focused ion beam process (FIB) to short-circuit the Au films on the two surfaces of the probe. Consequently, a homogeneous parallel-plate waveguide was formed, and microwave signals were able to propagate along the probe and emit from the tip apex of the M-AFM probe. It should be noted that the dimensions of the GaAs substrate and the Au films on the M-AFM probe determine the

Author complimentary copy. Redistribution subject to AIP license or copyright, see http://rsi.aip.org/rsi/copyright.jsp

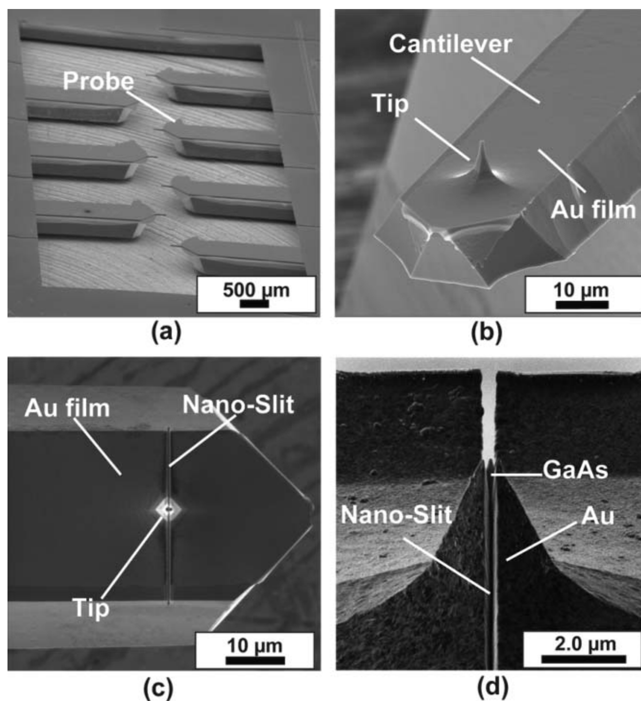

FIG. 3. SEM images: (a) the fabricated M-AFM probes; (b) the cantilever of the M-AFM probe; (c) the 100-nm-wide-FIB-fabricated nano-slit that is across the cantilever and through the center of the tip; and (d) high-magnification image of the tip.

characteristic impedance of the waveguide. To match the characteristic impedance of the associated transmission coaxial line, the waveguide is expected to have a characteristic impedance of 50 Ω. Thus, the cantilever and body of the M-AFM probe are designed with the dimensions of $250 \times 30 \times 15$ μm and $2740 \times 720 \times 340$ μm, respectively.

The SEM images of the fabricated M-AFM probes are depicted in Fig. 3(a). Figure 3(b) shows the as-fabricated cantilever of the M-AFM probe. The dimensions of the M-AFM probe depend on several small variations of experimental parameters, including the developing time of the resist pattern, the wet etching rate, and the electron beam (EB) evaporation rate. The average dimensions of the cantilever and the body of the M-AFM probes are typically $252 \times 31 \times 14$ μm and $2742 \times 723 \times 339$ μm, respectively. Thus, the characteristic impedance of the M-AFM probes is, on average, 49.3 Ω. Figure 3(c) depicts an SEM photograph of the FIB-fabricated nano-slit that has been patterned across the cantilever through the center of the probe tip. The observed tip is located near the front edge of the cantilever. As can be observed in Fig. 3(d), the tip is approximately 7 μm high, and the nano-slit is approximately 100 nm in width.

We prepared a sample for the scanning test of surface topography and microwave imaging. At first, a resist mask was patterned onto the glass substrate wafer by lithography. After developing the resist pattern, a 200-nm thick Au layer was deposited on the glass substrate by EB evaporation. Finally, the unexposed photoresists were lifted off in acetone. The resulting Au and glass step structure is depicted in SEM image shown in Fig. 4.

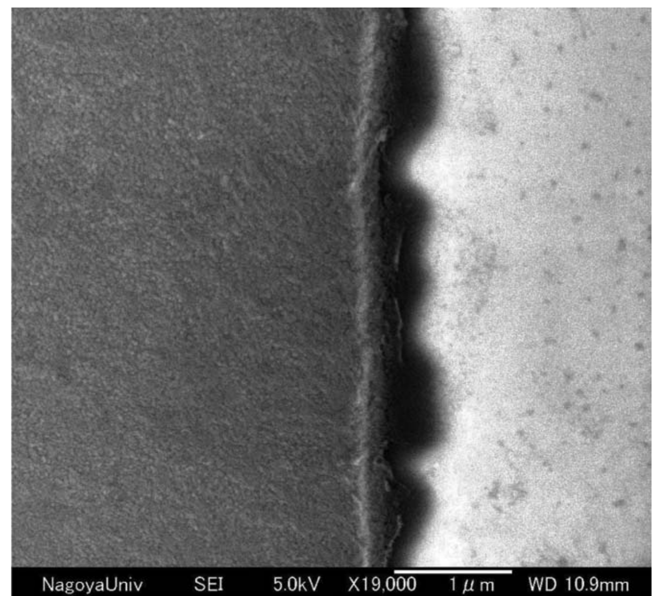

FIG. 4. SEM image of measured sample.

III. RESULTS AND DISCUSSION

Figure 5 depicts the M-AFM scanning results of the sample at the step area between the Au coating film and the glass wafer substrate. The M-AFM worked in noncontact mode, wherein the scanning speed was fixed to 5 μm/s, scanning area was 10 μm $\times$ 10 μm, environmental temperature was 24.5 °C, and the relative humidity was 38.4%. Figure 5(a) depicts the surface topography of the M-AFM-measured sample. In this image, the left side represents the Au film, whereas the right side is the glass substrate. As can be seen in the scanning profile depicted in Fig. 5(a), the thickness of the Au film was approximately 200 nm on average. In addition, Fig. 5(b) depicts the three-dimensional image with height

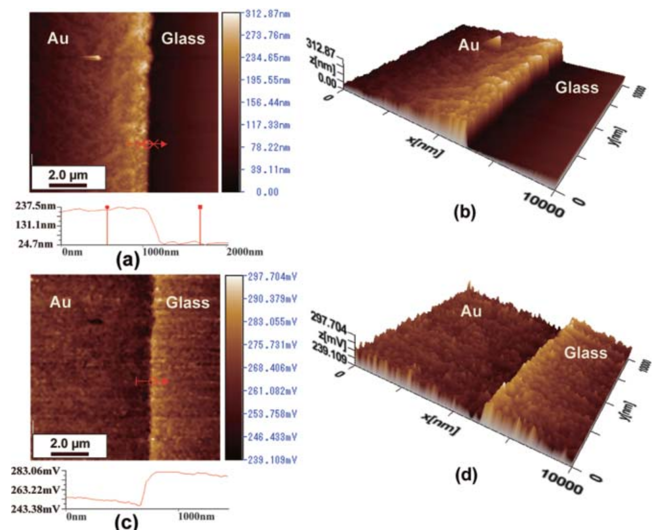

FIG. 5. (Color online) The scanning results that were obtained by the M-AFM: (a) AFM topography image of the Au/glass step sample; (b) a three-dimensional image that corresponds to (a); (c) microwave image of the output voltage that was converted from the measured microwave signals; and (d) a three-dimensional image that corresponds to (c).

Author complimentary copy. Redistribution subject to AIP license or copyright, see http://rsi.aip.org/rsi/copyright.jsp

information that corresponds to Fig. 5(a). Figure 5(c) depicts the microwave image of the voltage that was converted from the measured microwave signals, which were simultaneously acquired by the M-AFM probe at the corresponding position depicted in Fig. 5(a). Figure 5(d) depicts a three-dimensional image with electrical information that corresponds to that depicted in Fig. 5(c). This experimental result demonstrates that the microwave image has two spatial phases. Because the standoff distance between the tip of the M-AFM probe and the surfaces of the Au film and glass substrate is constant and controlled by the atomic force, thus, the response of the microwave signals were observed to change based on the different electrical characteristics of the measured materials. As per Fig. 5(c), the output voltage over the glass area is larger than that over the Au area, because the scanning started from the Au area with the initial offset from the nulling operation.

An analysis of the scanning profile depicted in Fig. 5(c) demonstrates that the spatial resolution is higher than 120 nm, and that the output voltages measured over the Au and glass areas were 262.5 and 281.7 mV, respectively. The difference between the measured voltages between the Au and glass areas is 19.2 mV. Since, the stability of the measurement is high, this value is large enough for evaluating the electrical properties of other materials having the conductivity between Au and glass. Based on the evaluation method of microwave measurement,[32] taking two different samples as the reference, the M-AFM should allow us to scan the electrical conductivities of other materials on a nanometer scale. In addition, based on the same principle, it can also be used to measure the permittivities of dielectric materials on a nanometer scale.

IV. CONCLUSIONS

We have created an M-AFM-obtained microwave image using a compact microwave instrument that was optimally synchronized with an AFM scanner. The distinguishing features of M-AFM are its ability to maintain a constant standoff distance between the probe tip and the sample surface and to measure the microwave signal interacted with the sample. Therein, both the topography and electrical-property images of the sample can be simultaneously characterized. Therefore, M-AFM is able to measure, *in situ*, the distribution of electrical properties on a nanometer scale. As shown in the experimental results, we successfully generated a microwave image of a 200-nm Au film coating on a glass wafer substrate with a spatial resolution of 120 nm, and, moreover, we measured the voltage difference between these two materials to be 19.2 mV. We believe that the high spatial resolution and simultaneous measurement capability of this M-AFM system will have important implications to nanotechnology characterization in the immediate future.

ACKNOWLEDGMENTS

This work was supported by the Japan Society for the Promotion of Science under Grants-in-Aid for Scientific Research (A) 20246028 and (S) 18106003.

[1] G. Binnig, C. F. Quate, and C. Gerber, Phys. Rev. Lett. **56**, 930 (1986).
[2] Y. Martin, D. W. Abraham, and H. K. Wickramasinghe, Appl. Phys. Lett. **52**, 1103 (1988).
[3] B. S. Li, B. D. Sattin, and M. C. Goh, Nano Lett. **6**, 1474 (2006).
[4] J. Tang, G. Yang, Q. Zhang, A. Parhat, B. Maynor, J. Liu, L. C. Qin, and O. Zhou, Nano Lett. **5**, 11 (2005).
[5] H. Kado and T. Tohda, Appl. Phys. Lett. **66**, 2961 (1995).
[6] J. W. Jang, R. G. Sanedrin, D. Maspoch, S. Hwang, T. Fujigaya, Y. M. Jeon, R. A. Vega, X. D. Chen, and C. A. Mirkin, Nano Lett. **8**, 1451 (2008).
[7] M. Nonnenmacher, M. P. O'Boyle, and H. K. Wickramasinghe, Appl. Phys. Lett. **58**, 2921 (1991).
[8] K. P. Puntambekar, P. V. Pesavento, and C. D. Frisbie, Appl. Phys. Lett. **83**, 5539 (2003).
[9] J. J. Kopanski, J. F. Marchiando, and J. R. Lowney, J. Vac. Sci. Technol. B **14**, 242 (1996).
[10] J. Smoliner, W. Brezna, P. Klang, A. M. Andrews, and G. Strasser, Appl. Phys. Lett. **92**, 092112 (2008).
[11] A. Olbrich, B. Ebersberger, and C. Boit, Appl. Phys. Lett. **73**, 3114 (1998).
[12] D. G. Xu, G. D. Watt, J. N. Harb, and R. C. Davis, Nano Lett. **5**, 571 (2005).
[13] J. E. Stern, B. D. Terris, H. J. Mamin, and D. Rugar, Appl. Phys. Lett. **53**, 2717 (1988).
[14] Z. H. Hu, M. D. Fischbein, and M. Drndić, Nano Lett. **5**, 1463 (2005).
[15] Y. Ju, K. Inoue, M. Saka, and H. Abé, Appl. Phys. Lett. **81**, 3585 (2002).
[16] Y. Ju, Y. Hirosawa, H. Soyama, and M. Saka, Appl. Phys. Lett. **16**, 162102 (2005).
[17] M. Tabib-Azar, N. S. Shoemaker, and S. Harris, Meas. Sci. Technol. **4**, 583 (1993).
[18] F. Duewer, C. Gao, I. Takeuchi, and X. D. Xiang, Appl. Phys. Lett. **74**, 2696 (1999).
[19] D. E. Steinhauer, C. P. Vlahacos, F. C. Wellstood, S. M. Anlage, C. Canedy, R. Ramesh, A. Stanishevsky, and J. Melngailis, Appl. Phys. Lett. **75**, 3180 (1999).
[20] Y. Ju, M. Saka, and H. Abé, IEEE Trans. Instrum. Meas. **50**, 1019 (2001).
[21] X. Y. Zhang, X. C. Wang, F. Xu, Y. G. Ma, and C. K. Ong, Rev. Sci. Instrum. **80**, 114701 (2009).
[22] M. Tabib-Azar and Y. Q. Wang, IEEE Trans. Microwave Theory Tech. **52**, 971 (2004).
[23] A. Karbassi, D. Ruf, A. D. Bettermann, C. A. Paulson, D. W. Van Der Weide, H. Tanbakuchi, and R. Stancliff, Rev. Sci. Instrum. **79**, 094706 (2008).
[24] Y. Q. Wang, A. D. Bettermann, and D. W. Van Der Weide, J. Vac. Sci. Technol. B **25**, 813 (2007).
[25] W. Kundhikanjana, K. J. Lai, H. L. Wang, H. J. Dai, M. A. Kelly, and Z. X. Shen, Nano Lett. **9**, 3762 (2009).
[26] K. J. Lai, H. L. Peng, W. Kundhikanjana, D. T. Schoen, C. Xie, S. Meister, Y. Cui, M. A. Kelly, and Z. X. Shen, Nano Lett. **9**, 1265 (2009).
[27] Y. Ju, T. Kobayashi, and H. Soyama, Microsyst. Technol. **14**, 1021 (2008).
[28] Y. Ju, M. Hamada, T. Kobayashi, and H. Soyama, Microsyst. Technol. **15**, 1195 (2009).
[29] A. Hosoi, M. Hamada, A. Fujimoto, and Y. Ju, Microsyst. Technol. **16**, 1233 (2010).
[30] Y. Ju, H. Sato, and H. Soyama, Proc. InterPACK2005 (CD-ROM), IPACK2005-73140 (2005).
[31] Y. Ju, T. Kobayashi, and H. Soyama, Proc. InterPACK2007 (CD-ROM), IPACK2007-33613 (2007).
[32] L. S. Liu and Y. Ju, Rev. Sci. Instrum. **81**, 124701 (2010).

Author complimentary copy. Redistribution subject to AIP license or copyright, see http://rsi.aip.org/rsi/copyright.jsp